

Tissue spectroscope: a novel *in vivo* approach to real time monitoring of tissue vitality

Avraham Mayevsky

Bar-Ilan University
Faculty of Life Sciences
Ramat Gan 52900, Israel
and
Vital Medical Ltd.
Petach Tikva 49170, Israel

Tamar Manor
Eliyahu Pevzner
Assaf Deutsch
Revital Etziony
Nava Dekel

Alex Jaronkin
Vital Medical Ltd.
Petach Tikva 49170, Israel
E-mail: mayevsa@mail.biu.ac.il

Abstract. Optical monitoring of various tissue physiological and biochemical parameters in real-time represents a significant new approach and a tool for better clinical diagnosis. The Tissue Spectroscope (TiSpec), developed and applied in experimental and clinical situations, is the first medical device that enables the real-time monitoring of three parameters representing the vitality of the tissue. Tissue vitality, which is correlated to the oxygen balance in the tissue, is defined as the ratio between O₂ supply and O₂ demand. The TiSpec enables the monitoring of microcirculatory blood flow (O₂ supply), mitochondrial NADH redox state (O₂ balance), and tissue reflectance, which correlates to blood volume. We describe in detail the theoretical basis for the monitoring of the three parameters and the technological aspects of the TiSpec. The comparison between the TiSpec and the existing single parameter monitoring instruments shows a statistically significant correlation as evaluated *in vitro* as well as in various *in vivo* animal models. The results presented originated in a pilot study performed *in vivo* in experimental animals. Further research is needed to apply this technology clinically. The clinical applications of the TiSpec include two situations where the knowledge of tissue vitality can improve clinical practice. The major application is the monitoring of “nonvital” organs of the body [i.e., the skin, gastrointestinal (G-I) tract, urethra] in emergency situations, such as in the operating rooms and intensive care units. Also, the monitoring of specific (vital) organs, such as the brain or the heart, during surgical procedure is of practical importance. © 2004 Society of Photo-Optical Instrumentation Engineers. [DOI: 10.1117/1.1780543]

Keywords: multiparametric monitoring; laser Doppler flowmetry; mitochondrial function; reduced nicotinamide adenine dinucleotide redox state; real-time tissue vitality; tissue spectroscopy.

Paper 02077 received Nov. 7, 2002; revised manuscript received Sep. 2, 2003, and Dec. 22, 2003; accepted for publication Feb. 24, 2004. This paper is a revision of a paper presented at the SPIE Conference on Optical Fibers and Sensors for Medical Applications, Jan. 2002, San Jose, CA. The paper presented there appears (unreferenced) in SPIE Proceedings Vol. 4616.

1 Introduction

The monitoring of tissue or organ vitality in real time is a critical factor in the process of surgery as well as in preoperative and intensive care unit management.

Currently, the main monitoring devices available for clinical use are aiming to provide hemodynamic and respiratory parameters.¹ Local monitoring of tissue parameters is very rare or absent in clinical routine, and most of the monitoring effort has been made in animal experiments. The multiple organ dysfunction syndrome accounts for most deaths in the intensive care unit,¹ and inadequate tissue perfusion and oxygenation are likely to contribute to the development of organ failures. Also, Fink² claims that “several lines of evidence indicate that cellular energetics are deranged in sepsis, not by inadequate tissue perfusion but rather by impaired mitochondrial respiration.” Therefore monitoring of parameters indi-

cating tissue perfusion and mitochondrial function is necessary for the improvement of patient outcome.

Presently, monitoring of mitochondrial function by monitoring NADH fluorescence *in vivo* has not been possible in clinical practice due to the absence of a Food and Drug Administration (FDA) approved device. The main aim of the present publication is the introduction of a new device—the Tissue Spectroscope—whereby tissue perfusion and mitochondrial function are monitored in real-time. Before going into details, a short introduction to tissue energy metabolism will be given.

Note that in this paper, we examine several pathophysiological conditions, defined as follows:

1. Ischemia is a decrease in blood supply to the tissue due to obstruction or constriction of a blood vessel.
2. Hypoxia is a decrease in the level of oxygen in the breathing mixture to which the animal is exposed.

Address all correspondence to Avraham Mayevsky, Bar Ilan Univ., Faculty of Life Sciences, Ramat Gan 52900, Israel; Tel: 972-3-5318218; Fax: 972-3-6354459; E-mail: mayevsa@mail.biu.ac.il

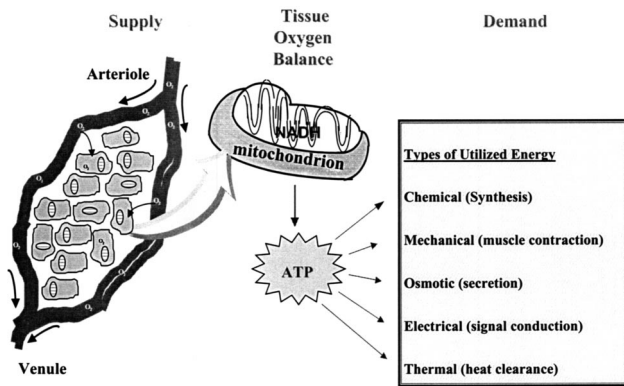


Fig. 1 Schematic representation of the way cells are able to do work. The blood supply is the source for the substrate and O_2 , providing the energy needs of the tissue. There exists a tissue oxygen balance, which can be defined as a ratio between the oxygen supply and demand. Every tissue may utilize the energy for various types of activity (the demand). Most of the ATP is synthesized in the mitochondria in oxidative phosphorylation.

3. Anoxia is a reduction in the level of oxygen to 0% by exposing the animal to 100% N_2 .
4. Hypoxemia is a decrease in the amount of oxygen in the arterial blood.

1.1 Tissue Energy Metabolism

The functional capacity of a tissue is related to its ability to perform its work. It is possible to assess this ability through the knowledge of changes in the oxygen balance, i.e. the ratio of oxygen supply to oxygen demand in the tissue.

Let us first briefly describe how cells are able to do work (Fig. 1). Healthy tissue cells perform various types of work, such as muscle contraction, secretion, the nervous system activity, and the synthesis of cell constituents. The energy needed to perform these types of work is derived from the degradation of foodstuffs, primarily through biological oxidation reactions, mediated by a respiratory chain comprised of several complex enzyme systems, in which oxygen is the ultimate electron acceptor. The electron transfers (oxidations/reductions) down the respiratory chain result in the production of energy-rich pyrophosphate bonds of adenosine triphosphate (ATP). Concomitantly with the electron transport, the respiratory chain components switch between reduced and oxidized states, each of which has different spectroscopic properties. Hydrolysis of the pyrophosphate bonds provides the energy necessary for the cell's work.

The formation of the pyrophosphate bonds depends on the sufficiency of sugar and oxygen supply to the tissue by the blood stream. Without the sufficient supply, cells cannot function properly and can, ultimately, die. Since most of the energy consumed by tissues is dependent on the availability of oxygen, the terms "energy" and "oxygen" are used here synonymously.

In a normal healthy tissue, the ratio—or balance—between oxygen supply and oxygen demand is positive and reflects the cell's functional capacity to do work. That is, the supply mechanism (oxygenated blood circulation) is able to provide the amount of O_2 needed for the demand mechanisms (ATP production for various types of work).

The Tissue Spectroscopy (TiSpec) monitors the parameters related to oxygen (energy) supply and oxygen (energy) demand.

1. Oxygenated blood availability represents the supply aspect and its measurement relies on the specific optical properties of static and moving blood cells.
2. On the part of demand, the spectroscopic properties of the respiratory chain components, unique to their redox status, are used as internal markers of the state of oxidative phosphorylation.

The intracellular concentration of mitochondrial NADH (the reduced form) is a parameter related to the tissue's state of energy metabolism. Energy exchange depends on pO_2 (partial oxygen pressure). Information regarding pO_2 in the tissue, therefore, is helpful for the evaluation of the tissue metabolic activity. The need for an intracellular pO_2 indicator, as a physiological and biochemical parameter of living tissue, has emerged more than 50 yr ago. Mitochondria are the intracellular organelles that consume most of the oxygen. Therefore, the redox state of electron carriers in isolated mitochondria as a function of oxygen concentration has been extensively studied (for a review see Ref. 3). Chance concluded that "For a system at equilibrium, NADH is at the extreme low potential end of the chain, and this may be the oxygen indicator of choice in mitochondria and tissue as well."

In excitable tissues, such as brain or muscle tissue, as well as in other cells, the activity of Na-K-ATPase is very sensitive to alterations in ionic homeostasis. An increase in extracellular potassium ion concentration, $[K^+]$, will stimulate pumping activity in order to bring the extracellular $[K^+]$ back to normal levels (i.e., 3-mM range). The activation of Na-K-ATPase will increase the hydrolysis of ATP and thus the mitochondria will phosphorylate the ADP molecules that are released. The accelerated activity of the mitochondria will be accompanied by a more oxidized state of the respiratory chain components, as well as by an increase in oxygen consumption.

To deliver more oxygen to the cells, blood flow and blood volume will be increased, and thus the extra oxygen needed by the tissue will be provided. This coupling between energy consumption and energy production is maintained as long as the O_2 supply is well regulated.

Under conditions where the oxygen supply or delivery is limited, e.g., after a stroke or heart attack, the energy supplier, i.e., the mitochondria, will not be able to produce the amount of ATP needed. As a result, energy-demanding processes will be restricted. The net effect of the imbalance between energy demand and supply will be manifested by a decrease in the tissue's ability to do work. This can lead to the development of various pathological deviations.

1.2 Real-Time Monitoring of Tissue Vitality

The monitoring of various tissue parameters is among the tools employed by clinicians to improve diagnosis. The major techniques developed for real-time analysis of tissue vitality are shown in Fig. 2. Their classification is based on the extent of the technology/probe invasiveness in the tested tissue.

Real Time Monitoring of Tissue Metabolic Activity and Vitality in Medical Practice

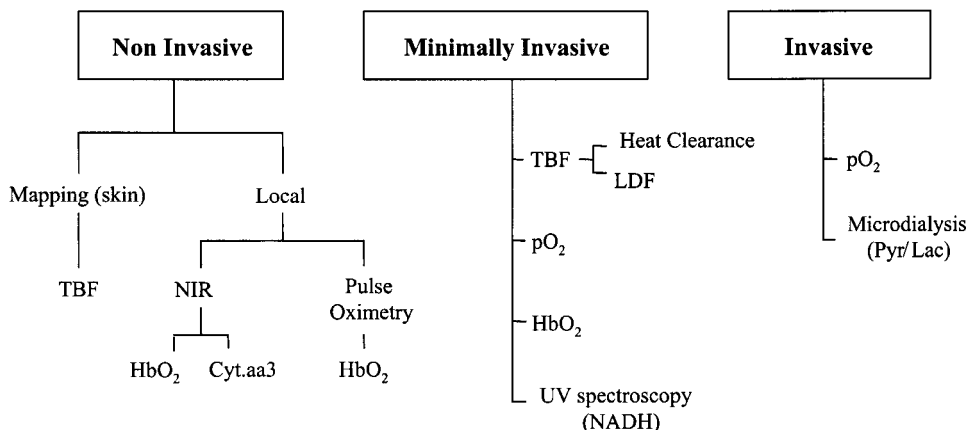


Fig. 2 Various techniques for real-time monitoring of tissue vitality currently available for clinical studies, classified according to their level of invasiveness (see text for details).

1.2.1 Noninvasive techniques

To evaluate the tissue hemodynamic and metabolic activity non-invasively and in real time, laser Doppler flowmetry (LDF) can be utilized. LDF provides information correlated to tissue microcirculatory blood flow^{4,5} (TBF). Another noninvasive approach is the use of a pulse oximeter that provides continuous data on hemoglobin saturation in the arteries of the monitored area (e.g., a fingertip). The development of the near-IR technology has opened up the possibilities of monitoring the saturation of hemoglobin and even the oxidation-reduction state of the mitochondria.⁶⁻⁸

1.2.2 Minimally invasive techniques

Our definition of this approach is that the monitoring probe has to be in contact with the examined tissue. This group of techniques includes the following four devices, as shown in Fig. 2.

Tissue blood flow (TBF)

To evaluate microcirculatory blood flow, at least two approaches have been developed and clinically applied. Heat clearance is the oldest one and requires heating of the sampled tissue to measure the heat clearance thereafter. The advantage of this technology is the ability to calibrate the flow in absolute units. However, the heating procedure is the main disadvantage of this approach. The predominant technology employed for monitoring the microcirculatory blood flow is LDF, which enables continuous monitoring without the need for tissue preheating. Its main drawback, according to most users, is that relative values are obtained instead of absolute values.^{9,10}

Oxygen partial pressure (pO₂)

Oxygen sensitive electrodes have been used since the early sixties and even earlier, in various *in vitro* as well as *in vivo* situations. Recently, continual monitoring of brain pO₂ has been implemented and a large number of clinical reports have been published.¹¹ Monitoring of pO₂ from the tissue surface

(for instance, during a surgical procedure) may be also affected by the surrounding atmosphere.

Saturation of hemoglobin

In order to determine the level of hemoglobin oxygenation in the circulating blood, a methodology was developed based on the absorption spectra of oxy and deoxy hemoglobin.¹²

Another approach, described by Rampil et al.,¹³ is based on two narrow wavelength windows that are used in a time-sharing reflectometer device. By this technique, only relative oxygenation values are monitored.

Mitochondrial NADH redox state

The conceptual foundations for mitochondrial NADH fluorometry were established¹⁴ and published in the early 1950s.

1.2.3 Invasive techniques

According to our definition, this group of techniques involves penetration of the monitoring probe into the tissue. The main disadvantage of this approach is the damage to the integrity of the monitored tissue. After the probe penetration, a new microenvironment is developed in the monitored area, and one must take this point into consideration.¹¹

1.3 Aims of This Study

The aims of this study can be summarized as follows.

1. We aim to describe the scientific and technological principles of the “TiSpec” whereby microcirculatory blood flow, tissue reflectance, and mitochondrial NADH redox state are measured by means of a single light source.
2. We intend to review the typical published papers on the monitored parameters under *in vitro* and *in vivo* conditions.
3. Since the TiSpec provides information on three different physiological and biochemical parameters, it was

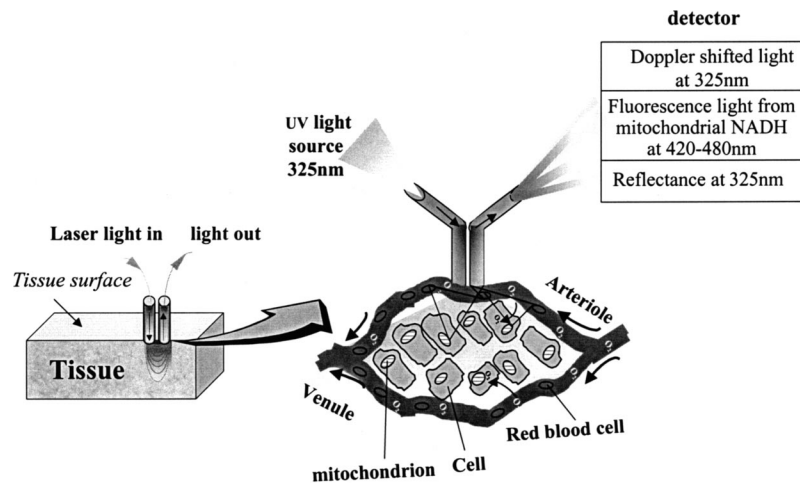


Fig. 3 Illustration of the experimental principles of the TiSpec simultaneous monitoring of TBF, tissue reflectance, and mitochondrial NADH redox status using the same light source and the same optic fibers.

necessary to compare it to various existing instruments, therefore this aim was divided to three stages, as follows.

- a. We aim to demonstrate the ability to measure NADH fluorescence signal comparable to a clinical fluorometer, by comparing measurements of aqueous NADH solutions at various concentrations by the TiSpec versus the Victor² 1420 Fluorometer.
- b. We intend to demonstrate the correlation between the TiSpec and the Victor² 1420 Fluorometer with respect to NADH fluorescence measurements in solution.
- c. We compare, in a short pilot study, the signals monitored *in vivo* by the TiSpec to those of standard *in vivo* monitoring devices by which tissue blood flow, NADH fluorescence, and reflectance are measured.

2 TiSpec

2.1 Principles of Monitoring

The TiSpec is an innovative monitoring device, developed by a commercial company, Vital-Medical Ltd., based on extensive longterm studies conducted by A. Mayevsky over the past 30 yr. It monitors continuous, real-time parameters that provide information related to the tissue's ability to perform its work. The principles of the TiSpec measurements, and their relation to the tissue's ability to perform its function are as follows.

The TiSpec uses a single light source to illuminate the tissue with UV excitation light, and detects light that is subsequently emitted from that tissue (Fig. 3). Light is conducted to and collected from the tissue by flexible optical fibers, combined in a single probe. The light emitted from the tissue contains three different components analyzed by the TiSpec:

1. *Doppler-shifted light at the wavelengths very close to the excitation wavelength.* This light is scattered by the moving red blood cells inside small blood vessels

(small arterioles, venules, and capillaries). Changes in this component are correlated with changes in the microcirculatory TBF.

2. *Fluorescence light (420–480 nm) emitted from excited intracellular NADH molecules.* Changes in the fluorescent signal intensity are correlated with changes in the intramitochondrial NADH redox state (Flu).
3. *Reflected light (R) at exactly the same wavelength as the excitation light.* This is also known as total back-scatter light. Changes in R are correlated mainly with blood volume changes in the tissue.^{13,15–21}

Changes in TBF, blood volume, and NADH redox state bring about changes in the emitted light signals. The principles and significance of the three different monitored parameters are described in the following.

2.1.1 TBF

The principle behind monitoring TBF by LDF is that coherent light from a laser source is delivered to the tissue under investigation by optical fibers. Photons that enter biological tissue undergo random scattering both by stationary tissue and by moving blood cells. Light that was scattered by moving blood cells undergoes a frequency shift due to the Doppler effect. A portion of scattered photons, both Doppler shifted and unshifted, is collected by the optic fibers and transferred to the detector. The Doppler-shifted light is superimposed with unshifted light on the photodetector. The photodetector produces dc levels related to the total back-scattered light (see later in the paper), while the ac ripple originates from the Doppler signal.²² To deduce the blood cell flux from the power spectra, Bonner and Nossal²³ proposed an algorithm based on the theoretical model of Doppler scattering.

Continuous real-time monitoring of TBF became possible after the development of the helium-neon (He-Ne) laser in 1961 by Javan et al.²⁴ Following a few years of fluid flow measurements,²⁵ the laser-Doppler velocimeter (LDV) was developed for blood flow measurements.²⁶ At the early stage,

the LDV was used for single vessel monitoring, and only in 1974 was Stern able to suggest the application of LDV for tissue measurement.^{27,28} The main steps in the development of the laser-Doppler blood flowmetry were described previously.^{22,29,30}

A wide range of tissues were tested^{9,10,22,23,28,31-33} by LDF. Usually, the changes in TBF are calculated as percent change as compared to a control level, defined as 100% of TBF. The LDF signal after death in animal studies is defined as 0% TBF. In many animal studies,³⁴⁻³⁶ as well as in the human brain,^{37,38} the output of the Doppler analyzer was very close to 0%. These definitions enable the calculation of relative changes between 0 and 100% TBF, and above, where the 0-mV value of the TBF analyzer was referenced as the 0% TBF.

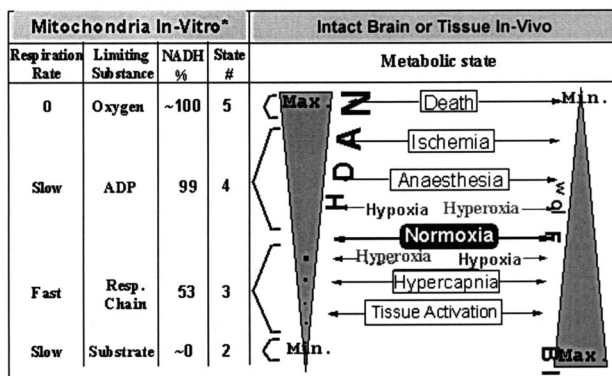
2.1.2 Mitochondrial NADH fluorescence

Only the reduced form of NAD⁺, i.e., NADH, absorbs UV light at almost the entire UVA spectrum area (315 to 400 nm), and fluoresces at 420 to 480 nm. A small part of the excitation light delivered to the tissue by the excitation optic fiber will be absorbed and reemitted as fluorescence by NADH. The total number of NAD⁺ and NADH molecules in a cell is constant, and any decrease in NADH will be accompanied by an increase in NAD⁺. Therefore, any change in the redox status of NAD⁺/NADH will be reflected in the intensity of the emitted fluorescence, while the more reduced state (NADH) shows more intense fluorescence than the oxidized state (NAD⁺). The reduced states, i.e., having higher NADH concentrations, have greater fluorescence intensities.

The redox state of NADH, and hence the fluorescence, depends on the availability of oxygen as well as on the rate of ATP turnover (ADP availability). When ATP consumption is constant, a decrease in intracellular O₂ shifts the redox potential to a more reduced state, thus increasing [NADH] and fluorescence intensity. When the O₂ level is 0, [NADH] accumulates to its maximal level. On the other hand, when [O₂] is not a limiting factor, any increase in ATP turnover (ADP availability) induces a shift in the mitochondrial NADH redox potential to a more oxidized state, thus decreasing the fluorescence signal intensity. Due to the dual dependence of the NADH redox state on O₂ availability and ATP turnover, the cause for a change in fluorescent signal is not unambiguous. However, combined with the information provided by TBF monitoring, a more accurate interpretation of the fluorescence changes can be accomplished.

There are two types of pyridine nucleotides (PNs), NAD⁺ and NADP⁺ (until 1964 these were called DPN and TPN, respectively). The spectroscopic as well as the fluoroscopic properties of the PN are being used in *in vitro* assays as well as for determination of intact cell energy metabolism. Very recently, Lübbers, a world leader in tissue metabolism research, concluded, "The most important intrinsic luminescence indicator is NADH, an enzyme of which the reaction is connected with tissue respiration and energy metabolism."³⁹

There is a general agreement on the characteristics of the spectra and their biochemical significance when measured *in vivo* and *in vitro*. The absorption and fluorescence spectra of NADH (the reduced form) have been well characterized at different levels of organizational complexity: in solution,⁴⁰⁻⁴³



* According to Chance & Williams 1955

Fig. 4 Schematic representation of tissue blood flow and NADH redox state *in vivo* responses to various perturbations, and the metabolic states of isolated mitochondria as defined under controlled conditions. In most perturbations, there is a negative correlation between blood flow and NADH redox state.

in cell suspension,^{44,45} in tissue slices,^{46,47} in perfused organs,⁴⁸ and under *in vivo* monitoring.^{21,49-51}

The conceptual foundations for tissue mitochondrial NADH fluorometry were established¹⁴ in the early 1950s. These defined various metabolic states of activity or rest for *in vitro* mitochondria. These metabolic states depend on the availability of oxygen, substrate and phosphate acceptor (ADP), and are associated with different redox states of NAD⁺/NADH.

During the past four decades, NADH fluorometry techniques have been developed, improved and applied to *in vivo* measurements in various organs. The principles of *in vivo* NADH monitoring are identical to the *in vitro* monitoring, though the interpretation of the results is different. As shown in Fig. 4, the *in vivo* NADH dynamic range is from minimum (corresponding to the *in vitro* state 2) to maximum (corresponding to the *in vitro* state 5), and it changes in a continuous manner rather than discretely between defined states. The brain is given as an *in vivo* example due to the relatively large amount of published material, yet the same scaling could be presented for other organs.

The awake brain is situated in the middle of the NADH range, i.e., between states 4 and 3. Any increase in the level of NADH indicates that the mitochondria are proceeding toward state 4 or 5. Activation of the brain results in a decrease in NADH and a shift toward state 3. In Fig. 4, selected metabolic conditions of the brain are shown covering the entire range of NADH responses.

The responses of mitochondrial NADH to metabolic perturbations have been studied in the brain as well as in other body organs.⁵² Jobsis and his group correlated the NADH fluorescence changes with the activation state of the brain and showed that convulsive activity,⁵³ direct cortical stimulation,¹⁶ or spreading depression⁵⁴ produced transient oxidation of NADH which was interpreted as a state 4-3-4 transition.

In 1975, the same group of investigators also introduced the measurement of cytochrome *a*, *a3* (by reflectance spectrophotometry) to study the brain *in situ*, in various functional conditions.^{6,55-57} Chance et al.³ have shown in detail that

NADH is the most oxygen sensitive component of the respiratory chain, and therefore is best to serve as an indicator of intracellular O₂ concentration and mitochondrial activity.

In 1972, the use of optical fibers in surface fluorometry was introduced, replacing the old “rigid” optical systems. As a result, measurement of NADH from the awake animal brain^{3,15} and from the heart became possible.⁵⁸

During the past 3 decades, this technique has been developed, improved and applied in many experimental setups in various organs *in vivo* and *in vitro*.^{17,18,34,44,48,59–68}

2.1.3 Total backscattered light-reflectance signal

Due to the scattering of excitation light by the tissue, some small part of the excitation light is reflected to the tissue surface, collected by the collecting fibers, and transmitted to the photodetector. This light intensity is referred to as backscattered or reflectance signal.

A certain amount of light is absorbed by the tissue (primarily due to hemoglobin). The absorption of light and the reflectance signals are inversely correlated.

Hemoglobin being the main absorption element, on blood elimination from the tissue, the reflected signal *R* increases dramatically. Conversely, when the tissue becomes more perfused with blood, *R* decreases. In this way, *R* provides information regarding blood volume in the tissue. This feature of the *R* signal also helps correct “artifacts” in the NADH fluorescence signal due to changes in tissue blood volume. When the blood volume changes, this affects both the accessibility of excitation light and the intensity of the fluorescent emission light. When the blood volume increases, the NADH signal decreases, and vice versa. Various algorithms, including *F/R* and *F-R*, have been used for correction. In the simplest case, the corrected fluorescence is expressed as a linear relationship between the measured fluorescence and the reflected excitation light.^{18–20,51,69–71} We have found that *F-R* provides good correction, therefore this correction technique was used both in the TiSpec (TS) and in the predicate laboratory fluorometer used for the *in vivo* comparative studies. This correction technique is necessary when NADH is monitored in a blood-perfused organ *in vivo*.

A large increase in *R* is measured *in vivo* (e.g., in the brain) upon animal death: oxygen is no longer available and a massive vasoconstriction occurs. This event of a large increase in the *R* signal, termed secondary reflectance increase (SRI), was described by Mayevsky and Chance,⁷² Mayevsky,⁷³ Mayevsky and Zarchin,⁷⁴ and Zarchin and Mayevsky.⁷⁵ In 1990, Mayevsky showed that SRI occurred when a large change in extracellular K⁺ was recorded.⁷⁶ Later we found that during the SRI, a decrease in blood volume is recorded.³⁶ The same principle applies when tissue absorption is increased due to vasodilatation and increased tissue blood volume. Under brain hypoxia, for example, the diminished O₂ induces elevation in the blood volume and the *R* signal drops as compared to the 100% control values. The same holds true when a high level of CO₂ (hypercapnia) induces a large increase in blood volume and a significant decline in the *R* signal.

Experimental results have clearly shown that changes in blood volume effect changes in the *R* signal. Those studies were summarized elsewhere.^{20,21}

2.1.4 Relationship between mitochondrial function and tissue microcirculatory blood flow

The mitochondrial metabolic state, in the concept of Chance and Williams,¹⁴ can be related to tissue blood flow and NADH redox state, as shown in Fig. 4. The responses of NADH or tissue blood flow to various disturbances are well documented.³⁵

If monitoring only one of the parameters, the information would be insufficient to determine whether a change in tissue vitality occurred. For example, if examining TBF alone, it would be impossible to know whether its decrease indicates a normal physiological response (to a factor such as lowered energy demand) or a pathological change such as ischemia. Likewise, NADH alone does not provide sufficient information regarding changes in the metabolic state. For example, if NADH declines (becomes more oxidized), it indicates an increase in oxidative phosphorylation. Without other data, it cannot be determined whether this is a normal response to hypercapnia (increased CO₂).

Once we measure changes in the NADH signal and correlate them to the changes in TBF, we can better identify the metabolic state that effected these changes. In this paper, we use the term hypoxia to describe a decrease in the partial pressure of O₂ in the inspired air, whereas ischemia is defined as a decrease in the blood flow to the tissue. Let us assume that a decrease in TBF is seen simultaneously with an increase in NADH. In other words, both the blood flow and oxidative phosphorylation have decreased. Depending on their magnitude, these changes could indicate a state of anesthesia, ischemia, or even death. If, on the other hand, we monitor simultaneously an increase in TBF, for example, in the brain, along with an increase in NADH (i.e., when the blood flow increases accompanied by a decrease in oxidative phosphorylation)—this would indicate a state of hypoxia. In other organs, such as the kidney under hypoxia, TBF is decreased and NADH is elevated. Further consideration of Fig. 4 clarifies the types of metabolic states that can be identified by changes in the measured variables.

2.2 TS—Technological Aspects

The TS device contains all the necessary sub-units for spectroscopic measurements of biological tissues. The Tissue Spectroscopy comprises a light source unit (LSU), a fiber optic probe, a detection unit (DTU), an analog-to-digital (A/D) and digital-to-analog (D/A) converter board, and a computer. The system is controlled by user-friendly software, which also enables processing, analyzing, and displaying the acquired data (see Fig. 5).

2.2.1 General instrument description

The TS can be better understood by examining its subunits. The light source is a He-Cd laser whose emitted light is directed to the tissue by a flexible optic fiber. The light interacts with the tissue and subsequently exits from the measured tissue volume. The light emitted from the tissue contains three components as already described, namely:

1. Fluorescent emission at 420 to 480 nm
2. Doppler-shifted laser light (325 nm)
3. total backscattered light (325 nm)

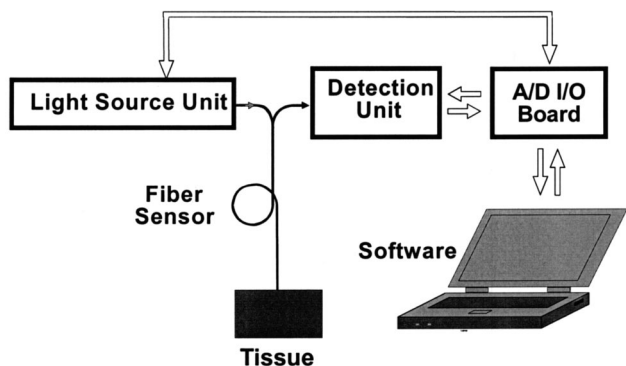


Fig. 5 TS system subunits. The LSU emits laser light into a fiber optic probe that delivers the light to the tissue and collects the returned light. The DTU converts light signals to electrical current, amplifies the signals, and performs Doppler detection. The A/D I/O board converts analog signals to a digital format for subsequent digital data processing by the PC.

The receiving optical fibers collect both the fluorescent and reflected signals and direct them to the detection unit. While the total backscattered light and the Doppler-shifted light have nearly the same wavelength of 325 nm, the fluorescence is red shifted toward 450 ± 30 nm. At the detection unit, a dichroic mirror separates the various reflected signals from the fluorescence. The dichroic mirror reflects the 325-nm reflected light toward a photodiode that produces the total backscatter and Doppler signals. The longer wavelength fluorescent signal passes through the dichroic mirror. This light is again filtered by a bandpass (420 to 480 nm) filter, and then enters a photomultiplier detector.

The photodetectors convert the light intensity to electrical signals. These electrical signals consist of two components: a dc component that is correlated to the total backscatter signal; and an ac component that is correlated to the Doppler signal. These signals are amplified and processed in the detection unit by the Doppler signal-processing subunit. The output of the Doppler processor is transmitted to an A/D converter. The A/D input-output (A/D I/O) board functions as an interface

between the instrument control software and other subunits of the instrument. This board is responsible for conversion of analog signals produced by the DTU into a digital form for further display and processing. It also supplies control signals to the LSU and to the DTU.

The system software is responsible for data acquisition, display, and storage along with control over all the instrument units. Additionally, it enables the user to control the instrument functions, and provides measured and calculated data.

2.2.2 Light source unit

The main part of the light source unit, shown in Fig. 6, is a Continuous Wave (cw) Helium-Cadmium (He-Cd) laser that comprises a laser head generating 325 nm light at 6 mW maximum power from Melles Griot (Carlsbad, California). The power supply is controlled by the TS software through the A/D I/O board. The laser is protected from unauthorized use by a key switch. The same key switch also protects the entire system from unauthorized use by shutting the power supply to the system.

A relatively high intensity laser was chosen since it has better light stability. This feature is important for the TS measurements. The outgoing 6-mW light from the laser head is attenuated to a very low light intensity when it exits the distal tip of the probe. The TS conforms to the safety guidelines for laser output by the ANSI Z136.1 standard Safe Use of Lasers. The instrument was designed in such a way that the mean excitation intensity for clinical applications was 0.5 mW/cm^2 , which is 0.5 of the threshold limiting values (TLVs). The TLVs also applied to the maximum permissible exposure (MPE) level (1 mW/cm^2). In the animal studies, the light intensity was in the range of 2.0 mW/cm^2 , which is 4 times the TLV.

After exiting the laser, the light passes through an acousto-optical modulator (AOM). This modulator chops the cw laser light with a duty cycle of 1/10. This chopping operation mode permits the usage of a synchronous detection scheme and enables additional reduction of the excitation intensity. The

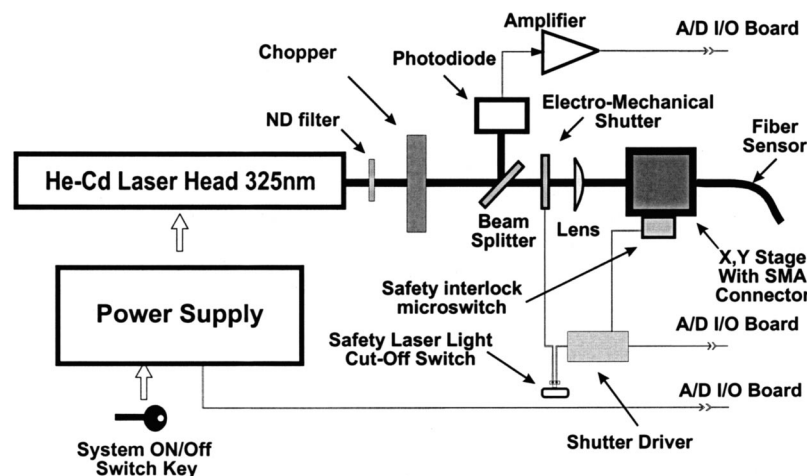


Fig. 6 LSU includes He-Cd laser head with laser power supply, neutral density (ND) filter, chopper, electromechanical shutter, beamsplitter, and photodiode for light intensity monitoring, and a lens for coupling the laser beam into the optic fiber which is connected by a SMA (subminiature version A) connector. Interlock and safety switches are installed for additional safety.

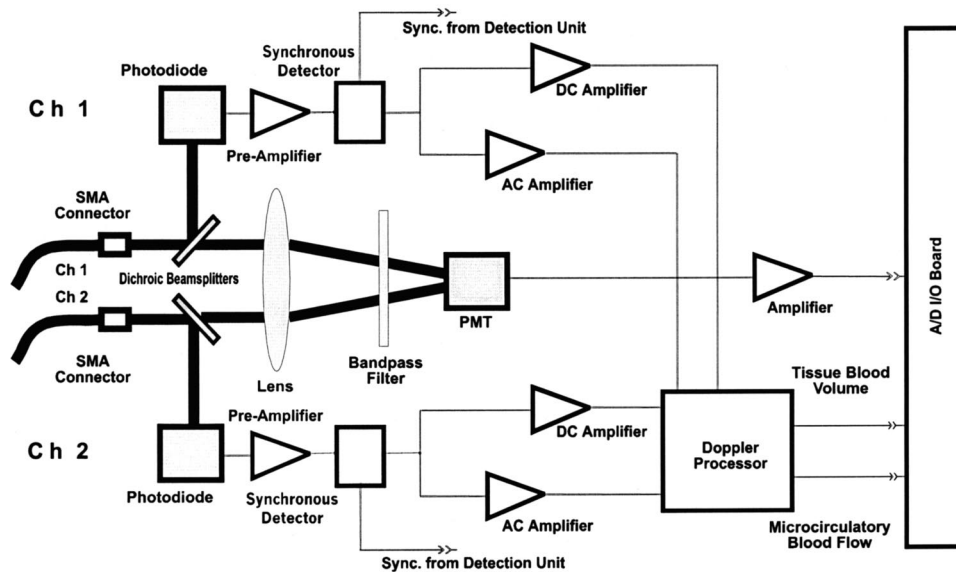


Fig. 7 DTU consists of two input channels (optic fibers) directed through beamsplitters into two photodiodes (for Doppler analysis) and one photomultiplier tube (PMT) for NADH fluorescence analysis.

same AOM enables excitation intensity control by the software.

The chopped light then passes through a beamsplitter that splits about 5% of the total light intensity toward the intensity monitoring photodiode. The monitoring photodiode transmits the light intensity correlated voltage to the A/D I/O board after appropriate amplification. This voltage is used to monitor the output intensity for both normalization and safety purposes.

After exiting the beamsplitter, the light passes through an electromechanical shutter. This shutter is controlled by the software through the A/D I/O board and is closed when the instrument is not monitoring.

At the final stage, the light beam is coupled to the optical fiber by means of a focusing lens and an x - y stage, connected to the fiber by an SMA connector. A safety interlock micro-switch is placed near the SMA connector, and precludes laser exposure unless the probe is connected.

2.2.3 Detection unit

The detection unit is built according to the two-channel concept (Fig. 7), which enables, by subsequent subtraction of the two channels, the elimination of all synchronous noises.⁷⁷ This arrangement enables efficient subtraction of noise originating in the laser light source, so that a longitudinal, multi-mode laser can be used for LDF measurements.

The two collecting optic fibers, at the detection unit end of the Y-shaped fiber optic probe, are connected to the detection unit by SMA connectors. The light of each channel passes through the dichroic beamsplitter. This beamsplitter separates backscattered and Doppler shifted light at 325 nm from NADH fluorescence light at 420 to 480 nm. Most of NADH fluorescence light passes through the beamsplitter, while the backscattered and Doppler-shifted signals are reflected toward the photodiode detectors, which convert them to a voltage signal.

The output of the detector is fed to a synchronous detector, which comprises sample and hold (S/H) circuit and appropriate filters (not shown in the figure). The synchronous detector enables the detection of the duty cycled light as generated by the LSU. The output of the synchronous detector is a combination of dc and ac voltages that are similar to those that would be acquired from a regular cw (non-duty-cycled) excitation.

The reflected light is a very slowly changing parameter and is, therefore, represented by the dc voltage level at the amplifier output. The Doppler-shifted light signal appears as ac ripple at the relatively high dc level. Both signals appear at the output of the synchronous detector. The Doppler signals pass through an ac amplifier, while the backscattered signals pass through a dc amplifier.

After amplification, both signals are fed to the Doppler processor. The Doppler processor output consists of two signals. The first signal is correlated to Doppler-shifted light that is due to microcirculatory TBF. The second signal is correlated to the backscattered light intensity that is relevant to tissue blood volume. When exiting the Doppler processor, both signal types are slow changing, with a time constant of ~ 3 s.

The light that passes through the dichroic beamsplitter of each channel is refracted toward a common detector by a lens. Before reaching the detector, the light passes through a bandpass filter that transmits only NADH fluorescence wavelengths (420 to 480 nm).

The fluorescence detector signals, after amplification, are transmitted to the A/D I/O board. The amplifier also operates as a synchronous detector by receiving the clock signal (not shown) from the clock unit. When exiting the fluorometer, the fluorescence signal is a slowly changing parameter, with a time constant of ~ 3 s. The output of the amplifier is connected to the A/D I/O board. The sampling rate for all three signals was 10 Hz.

2.2.4 TS performance

Since the excitation light of the TS is in the UV area (325 nm), light penetration is no greater than 1 mm. Most of the information is collected from a sphere having 0.6 to 0.7 mm in diameter. The stability of the three types of measurement was tested separately. The Doppler stability (tested in a solution of microspheres) was better than 1% per hour. The stability of the reflectance parameter was tested by applying the tip of the probe to the surface of Delrin (a standard inert plastic white material). The minimal detection capacity of the TS was 50 nW at 325 nm. The stability was better than 1% per hour. To test the fluorescence signal, we used a solution of NADH dissolved in a large volume of saline to avoid bleaching. The minimal sensitivity of the photomultiplier was 1 pW at 460 nm. The stability was better than 1% per hour. Regarding a possible error due to the placement of the probe, note that the only way to avoid such errors is to have a constant good contact between the tip of the probe and the tissue. If the probe is moved relative to the tissue, the measurement will start at a new baseline. Only tendency changes can be compared when the probe is moved during the measurement.

3 Methods and Materials

3.1 Basic Experimental Approach

3.1.1 *In vitro* measurement

The ability to quantitatively measure NADH fluorescence, comparable to a standard clinical fluorometer, is demonstrated by direct fluorescence measurements in aqueous NADH solutions, tissue, and blood. The fluorometric analysis of aqueous NADH solution by the TS provides a suitable simulation of fluorometric tissue analysis, since the principles of *in vitro* and *in vivo* NADH monitoring are identical. There is an agreement on the characteristics of NADH spectra and their biochemical significance, when measured both *in vivo* and *in vitro*. The intensity of the fluorescence band is independent of the organizational level of the environment and is proportional to the concentration of NADH (the reduced form).

3.1.2 *In vivo* measurements

The ability to measure TBF comparable to another laser Doppler flowmeter is demonstrated by simultaneous *in vivo* measurements of TBF in different tissues of rats and gerbils using the Tissue Spectroscope and the other commercial laser Doppler flowmeter. Metabolic perturbations were induced in the experimental animals, resulting in TBF alterations that were measured.

Additionally, to demonstrate the *in vivo* performance of the TS, we have compared the *in vivo* NADH signal measured by the TS with the measurements by a standard *in vivo* fluorometer currently used in academic research. Although the research fluorometers are not classified as medical devices, their effectiveness in carrying out *in vivo* fluorometric measurements is widely accepted. We felt that such comparison might be useful to further demonstrate the effectiveness of the TS.

3.2 Instrumentation

3.2.1 Monitoring and measurement devices

The *in vitro* fluorometer—Victor² 1420 (EG&G Wallac) is a multilabel, multitask plate counter, operating as a prompt fluorometer, time-resolved fluorometer, and a luminometer. For excitation of NADH, a 355-nm bandpass filter was used. The fluorescence emission was collected via a 460-nm bandpass filter. The excitation light was delivered to the sample from the up side. The emission light was also collected from the up side. This arrangement was necessary to ensure a short light path needed to eliminate sample autoabsorption.

The Laser Doppler Flowmeter used was the Periflux model PF 2B Laser Doppler Flowmeter, Sweden. The Perimed PF 308 (standard, multipurpose) probe was utilized. The laser Doppler flowmeter was calibrated according to the manufacturer's instructions.

The TS is described in Sect. 2.2.

The standard *in vivo* laboratory fluorometer was described in detail by Mayevsky and Chance²⁰ and Mayevsky.²¹

3.2.2 Fiber optic probes

The standard fiber optic probe [Fig. 8(a)] is composed of UV-enhanced fused silica fibers arranged in a bundle of excitation and emission fibers. The probe is designed for light transmission both from the laser toward the tissue (the excitation fiber) and from the tissue toward the detectors (the emission fibers). On the machine end, the probe is equipped with optical SMA connectors. On the tip end, the fibers are positioned and glued in a hypodermic stainless steel tube, where the emission fibers adjacently surround the excitation fiber [Fig. 8(a)]. For clinical usage, the probes were packaged in a thermoformed tray, sealed and sterilized by exposure to ethylene-oxide (Eto).

We developed three different types of disposable probes, designed for optical measurements of brain tissue vitality using the TS device. All these types have a similar fiber optic bundle, but feature different external design and accessories. The different types of probes were designed to enable the TS to monitor the brain tissue during different types of craniotomy and surgery.

TSP2000-2

This probe is designed for monitoring exposed brain cortex, in various locations under craniotomy. The bundle end is fitted with a thin metal tube accommodating the optical fibers [Fig. 8(b) panels 1 and 2].

The spatial position of the brain is dynamic. The brain pulses as a result of breathing and the blood flow pulsation. Since the probe is sensitive to movement, and monitoring of continuous brain vitality trends is required, the probe must remain in continuous contact with a certain measurement point on the brain. We overcome this difficulty by developing intermediate arms that, combined with the TSP2000-2 probe, enable the probe to track the changing height of the brain cortex. An adjustable floating arm [Fig. 8(b), panel 1] and an adjustable manipulator [Fig. 8(b), panel 2] were designed to handle the probe. Both attachments had to be applied to a standard flexible Yassergil arm, which is a common instrument in neurosurgery.

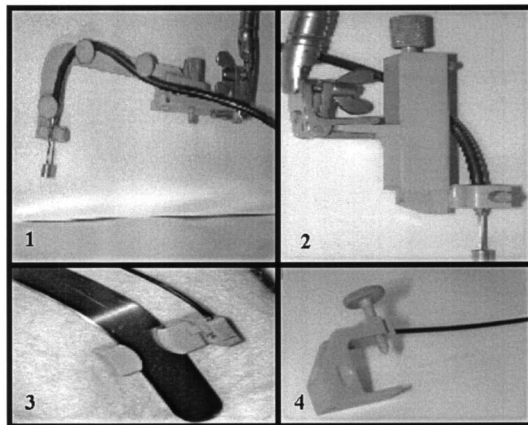
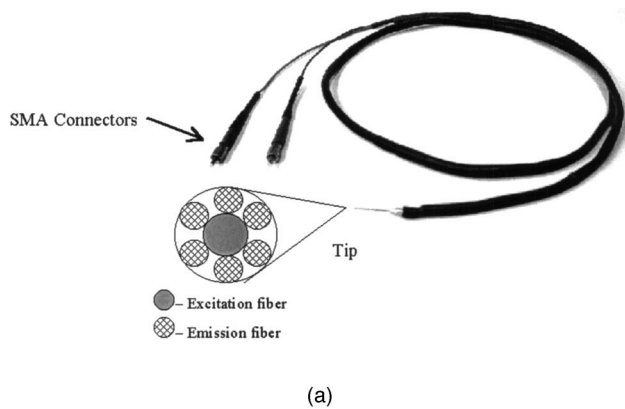


Fig. 8 Picture of a standard fiber optic probe (a) used to connect the *in vivo* monitored tissue to the TS, where the enlargement of the tip shows the arrangement of the excitation and emission fibers in the common part of the probe; (b) four clinical applications of the probe: 1, TSP2000-2 probe on floating arm; 2, TSP2000-2 probe on manipulator arm; 3, TSP-R1 probe and a slider attached to a neurosurgical retractor; and 4, TSP-C1 clamp type probe.

TSP-R1

This low-profile probe is designed for monitoring the metabolic stress of brain tissue pressed under a neurosurgical retractor, during profound surgery [Fig. 8(b), panel 3]. The probe is versatile and can be attached to various types of sliders to fit various widths of retractors commonly used in neurosurgery. The surgeon can easily click together the probe and the appropriate retractor attachment (slider). The elasticity of the slider enables a firm grasp of the retractor along with an adjustment of the probe location along the retractor. The bending radius of the fibers was decreased to 5 mm, resulting in a total height of 7 mm of the plastic probe.

TSP-C1

This miniature probe [Fig. 8(b), panel 4] is designed to monitor the exposed brain cortex, adjacent to craniotomy area. The fibers are sheathed within a thin flexible cable, equipped with a plastic clamp that is tightened upon the bone. In this probe, we succeeded, for the first time, in handling bending fibers without cracking them. The advantages of the TSP-C1 probe are its small dimensions and the direct attachment to the bone without any accessories.

3.3 Measurement Performance

3.3.1 *In vitro* measurements of NADH in solution

A series of solutions with known concentrations of NADH (β -nicotinamide adenine dinucleotide, the reduced form, Lot 128H7001, Sigma chemical, co. N-8129) in double-distilled water (DDW) were prepared. The samples were transferred into a microtitration plate with 96 wells for the measurements by the Victor² device. Every measurement was repeated twice for each duplicate, to obtain four reading values for each NADH concentration.

The same NADH solutions were placed in separate vials into which the “pencil type” probe (010) of the TS was placed. Fluorescence intensity was recorded by the TS, in millivolt units.

Our preliminary studies revealed that the range of 0 to about 180 μ M NADH in solution provides linear relationships with the fluorescence levels.

Statistical analysis

The millivolt fluorescence values of the TS, and the arbitrary units for the Victor² were plotted against concentration values. A linear plot is expected for the concentration range used. The regression line was calculated for each instrument separately. Additionally, a correlation test was performed between the fluorescence values as measured by each instrument at identical NADH concentrations. This was done to evaluate the similarity of the two instruments. A linear plot with a high correlation coefficient was expected.

Since there is no gold standard for these measurements, we also used the Bland and Altman^{78,79} analysis to compare the two instruments.

3.3.2 Animal preparation

Sixteen male Wistar rats (200 to 240 g) and 16 male Mongolian gerbils (*Meriones unguiculatus*) (45 to 55 g) were used. The rats were anesthetized by Equithesin (E-th = chloral hydrate 42.51 mg; magnesium sulfate 21.25 mg; alcohol 11.5%; propylene glycol 44.34%; pentobarbital 9.72 mg) intraperitoneal (IP) injection 0.3 ml/100 g body weight. The left femoral vein was cannulated for intravenous (IV) injections. The small intestine was exposed by a minimal opening in the abdomen to minimize dehydration and loss of body heat. The exposed segment of the small intestine was placed on a tray and, except for the area covered by the probes, covered to maintain humidity. The probes (TS and PF308, Perimed) were held together (with the probe tips at the same height and 2 mm apart) by a flexible arm clamp and positioned on the surface of the intestine. The probe tips lightly touched the intestine surface, and care was taken not to apply excess pressure. The animals were kept anesthetized during the operation as well as during the entire monitoring period, by IP injections of E-th 0.1 ml every 30 min. We have been using this anesthetic for approximately 25 yr and it has never shown significant effects on mitochondrial activity. Furthermore, we have not been able to change the response of the rat brain to spreading depression by using an increased dose of equithesin, suggesting that this is a safe drug.⁸⁰ The addition of small volumes of E-th every

Table 1 The distribution of the various perturbations in various organs and animals.

Animal	Organ	Perturbation		
Rat	Intestine	Short anoxia <i>n</i> = 16	Anoxia <i>n</i> = 16	Cardiac arrest <i>n</i> = 14
Gerbil	Brain	Anoxia <i>n</i> = 16	Ischemia <i>n</i> = 12	Terminal anoxia <i>n</i> = 10

30 min kept the animal in a stable state. Body heat was measured by a rectal probe (YSI) and was regulated to be at the range of 35 to 37 °C using a heating blanket.

The gerbils were anesthetized by Equithesin (E-th) IP injection of 0.3 ml/100 g body weight and placed in a head holder. After a midline incision of the skin, a hole (5 mm in diameter) was drilled in the parietal bone of the left hemisphere. The dura mater remained intact. Two stainless steel screws in the right parietal bone were used, with dental acrylic cement, to fixate the probes, which were positioned by a micromanipulator on the cortex. The two common carotid arteries were isolated just before brain surgery, and ligatures of 4-0 silk threads were placed around them. Body heat was measured by a rectal probe (YSI) and was regulated to be at the range of 35 to 37 °C using a heating blanket. The animals were kept anesthetized during the operation as well as during the entire monitoring period, by IP injections of E-th 0.03 to 0.05 ml every 30 min.

3.3.3 Metabolic perturbations

In the reported study, TBF and NADH in rat intestine (16 animals) and gerbil brain (16 animals) were monitored *in vivo*, simultaneously, by the TS and Perimed or standard *in vivo* fluorometer, while systemic perturbations were induced in the animals. The two probes were attached together (tips at the same height) and placed on the tissue, so to simultaneously measure the TBF and NADH of the tissue under the probes. In these animal studies, the light intensity at the probe tip did not exceed 1.3 mW. Under the present experimental conditions, we did not observe any obvious damage to the tissue. The intestine was not sensitive to the UV light, and the brain was protected by the dura mater.

There were three levels of comparison:

1. different sites in the same tissue by the two instruments
2. different tissues
3. different species of animals

Due to the distance between the locations of the two probes in the same tissue, we did not compare two points of measurement by the same instrument because of the obvious difference between the optical characteristics of the tissue. If the same probe is located on different portions of the tissue or organ, the difference in baseline values will be larger than the response to several perturbations, therefore only tendencies are compared at the same site.

The experimental animals were exposed to the following perturbations (the distribution of the various perturbations in the organs and animals are shown in Table 1):

1. *Anoxia*: The animals were exposed to oxygen deficient atmosphere by spontaneous breathing of N₂, for a short (10-s) or long (25-s) period. Terminal anoxia was induced by 100% N₂ until the animal stopped breathing.
2. *Cardiac arrest*: To induce cardiac arrest, an overdose of anesthetics (Equithesin) was injected IV.
3. *Ischemia*: Reversible occlusion (~1 min) of the two common carotid arteries (by constricting them with threads) led to brain ischemia in the gerbils.

Experimental protocols

Monitoring commenced at 30 min postoperation. Perturbations were then applied to the animals (a specific marker was entered to the computer), following the protocol of each individual experiment.

3.3.4 Data collection, analysis, and statistics

Data collection

The TS and Perimed display relative values of the blood cell flux and are not calibrated in absolute physiological units. The flux time constant for both instruments is ~3 s. The range of the recorder output is 0 to 10 V. The blood cell flux values are shown in percent units (percent of the blood flux corresponding to a full scale deflection, i.e., the adjustment yielding a full scale deflection at 10 V). CF and *R* are also measured by the TS and the standard *in vivo* fluorometer. The data were collected at a rate of 10 samples/s, stored, and saved in different channels of a computerized data acquisition program. The values were viewed on the screens and plotted in a chart during the experiment. All the calculations are presented as the average percent change from baseline levels (100%). Each perturbation was initiated at the time when the monitored parameters were at a particular baseline value (in percents). The event was noted on the computer record by a marker entered at the moment of the perturbation commencement. For the TBF parameter, each animal started at its own, unique baseline level. For NADH, the initial baseline was always defined as 100%.

Data analysis

The TS TBF channel was passed through a running median filter for smoothing (± 50 samples) to reach a noise level similar to that of the Periflux signal (the signal of the Periflux PF 2B is passed through various filters before being extracted). The signals from the TS NADH channel and the standard *in vivo* fluorometer NADH channel were both passed through a running median filter (\pm five samples) to reduce the noise level. The running median filter returns the median number of a specified set (in the case of TS TBF—100 data points) so that 50 data points are below it and 50 data points are above it. Starting from the first number of the set, the first median value is provided for data points 1 to 100, the second is for data points 2 to 101, the third for data points 3 to 102 and so on (running). The running median filter smoothes extreme single data points, usually defined as instrument noise, and displays the original recorded data points.

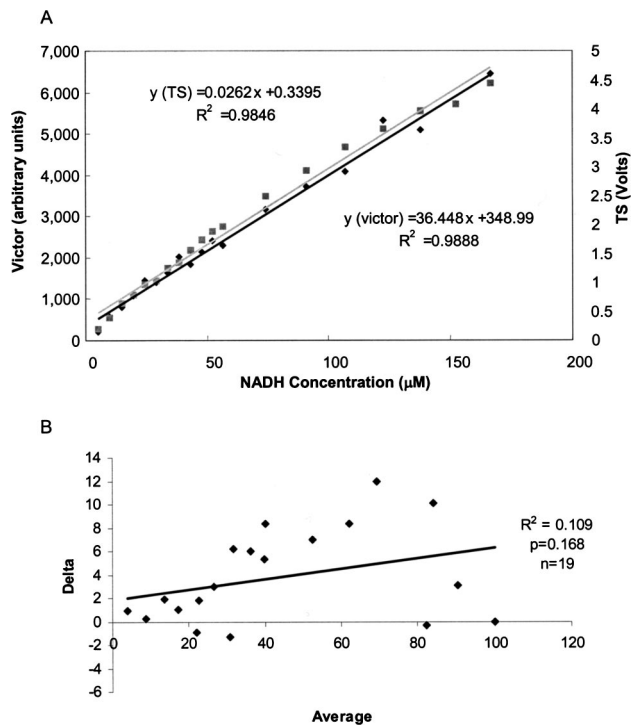


Fig. 9 (a) Readings of the TS (on the right Y axis), and readings of the Victor² (on the left Y axis) plotted against NADH concentrations. A linear regression was calculated for each instrument, and the equation and R^2 are presented. (b) The difference (delta) against the average for the tested instrument (TS) and the standard instrument (Victor²).

Statistical analysis

The correlation coefficient (r) between the values measured by the TS and the PF 2B was calculated for each event, starting at the time of the marker entrance, for 2 min with a total of 1200 data points (anoxia, terminal anoxia, and ischemia) or for 80 s with a total of 800 data points (short anoxia).

The Fisher z transformation was applied to determine the confidence intervals for each event. Each r was transformed and a confidence interval was computed on the z scale. Thereafter, the confidence limits were transformed back to obtain a confidence interval for r .

An average correlation coefficient (r_{average}) was calculated by averaging the z values to obtain a z_{average} for all animals in each type of event in each species, and then transforming it back. The confidence intervals for r_{average} were computed from the confidence intervals of the z_{average} .

4 Results

4.1 *In Vitro* Measurements of NADH Solution

Linear correlation coefficients were calculated, in which values close to 0 describe variables that are essentially uncorrelated and values close to 1 describe those that are highly correlated. The results of the readings of the TS and the Victor² plotted against NADH concentrations are presented in Fig. 9(a). Linear regression was calculated for each instrument and the linear equation and r^2 are presented in the graph.

The correlation coefficients between Victor², TS, and NADH concentration (C), were high:

$$r(\text{Victor}^2, C) = 0.994, \quad r(\text{TS}, C) = 0.992.$$

The high degree of correlation implies the similarity of the two measurement systems. The coefficient of correlation between Victor² and TS was also calculated, $r = 0.9915$.

Figure 9(b) (the Bland-Altman plot) shows the difference against the average of the test and standard method measurements, with 95% limits of agreement (broken lines) and the regression line. As the two methods of NADH fluorescence measurement use different scale units, the measurements were normalized as percent of the maximal values observed. The mean difference (TS-Victor²=new-old) is 3.8% and the standard deviation (SD) is 4.00%. The correlation between difference and average is weak ($r^2 = 0.11$, $p = 0.17$ 95% CI from -4.04 to 11.64). The linear trend is very moderate and not statistically significant ($p = 0.167$). In the region of high absolute measurement values, the differences are small (3% or less). Thus, one can state that “the differences are small, and the new method can be applied.”

4.2 *In Vivo* Measurements

All measurements under *in vivo* conditions were conducted in slightly anesthetized animals. The injection of additional amounts of the anesthetic material did not affect the monitored signals. Only large doses of E-th that may decrease systemic blood pressure, will affect the monitored signals. The nature of the responses is clearly appreciated from the average responses. Figures 10 and 11 present the time plot graphs of the blood flow and NADH responses measured by both instruments, averaged over all the experiments, for each animal type for several perturbations.

Note that in Figs. 10 and 11, the curves of the TBF obtained by the TS and the commercial device are not overlapping due to the differences in the calibration of the two devices. The units presented in the TBF scale are relative and have meaning only when tendencies recorded in real time are compared. On the other hand, the NADH is calibrated in the same way in both the TS and the laboratory fluorometer. To compare the LDF values, it is possible to normalize the values to 100% at the perturbation onset. Since our comparative analysis was performed through correlation analysis, the use of this normalization technique was of no importance.

Figures 10 and 11 (left) show the measurement results in the gerbil brain that reflect autoregulatory and metabolic responses to anoxia and terminal anoxia.

Figure 10 (left) shows the response of TBF and NADH to anoxia. As it is seen, the initial change due to anoxia is an increase in the NADH level. This is due to the decrease in the oxygen available to the brain mitochondria, which shifts the $[\text{NAD}]/[\text{NADH}]$ ratio toward a more reduced state. Concomitantly, as we see, there is an initial autoregulatory decrease in the TBF due to the change in blood pressure. This is followed by an increase in TBF when the animal is allowed to breathe air again.

The initial change in the parameters in response to ischemia (not shown in the graphs) was a decrease in TBF. This resulted from the occlusion of the common carotid arteries. The decrease continued until reopening of the arteries. The response of the mitochondrial NADH commenced after the initial drop in the blood flow and returned to the preischemic level after the reperfusion.

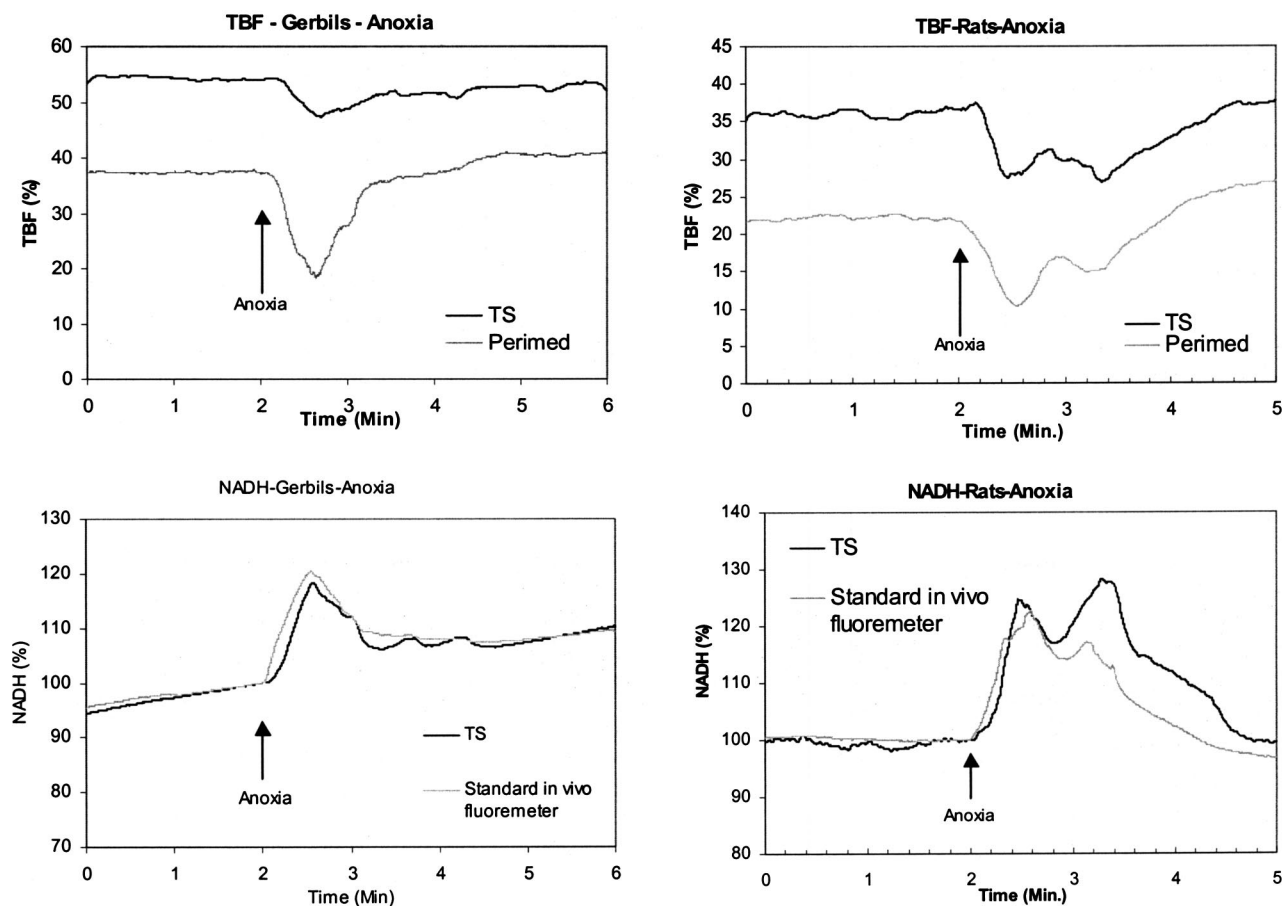


Fig. 10 Responses of the gerbil brain (on the left) and the rat small intestine (on the right) to reversible anoxia. Under anoxia, the NADH was elevated due to the lack of O_2 in the blood flowing to the organs.

Figure 11 (left) shows the results regarding brain TBF and NADH due to terminal anoxia. As we see, there is an increase in the NADH level due to the decrease in the available oxygen. Insofar as the gerbil eventually ceases to breathe, the NADH signal remains high. As seen in this figure, there is an initial decrease in TBF, as in anoxia. The autoregulatory effect is seen as a “shoulder” in the TBF decrease. Insofar as the gerbil eventually ceases to breathe, the TBF signal drops and remains low.

Figures 10 and 11 (right) show the results of measurements in rat small intestine that reflect hemodynamic and metabolic responses to anoxia and cardiac arrest.

The response of the intestine to anoxia, shown in Figure 10 (right), is a bi-physic decrease in TBF and a bi-phasic transient increase in NADH. This is similar to the responses to short anoxia, except that in short anoxia the effects are smaller and the TBF shows one phase response.

Figure 11 (right) shows the measurements of rat intestine TBF and NADH when exposed to cardiac arrest. As it is seen, the initial change due to cardiac arrest and the cessation of breathing is manifested by an increase in the NADH level. This is due to the decrease in the oxygen available to the cells mitochondria which shifts the $[NAD]/[NADH]$ ratio toward a more reduced state. Cardiac arrest causes the heart to cease pumping, which results in lower TBF. There is, understandably, no subsequent rise in TBF or decrease in NADH. Since

the heart stops pumping blood, no autoregulatory effect is possible and no “shoulder” is seen.

The changes due to anoxia in rat small intestine, as seen in Fig. 10 (right), are similar to those in the gerbil brain because they conform to the same physiological mechanisms, although the response of the TBF and NADH in the intestine is bi-phasic.

4.2.1 Correlation

The TBF measurements by the TS and Periflux 2B correlated well, with an average correlation coefficient $R^2=0.70$. The NADH measurements by the TS and the standard research *in vivo* fluorometer had an average correlation coefficient $R^2=0.86$. The averaged correlation coefficients for each animal type and each perturbation type are shown in Fig. 12.

4.2.2 Variance

Using SAS software, two variance analyses were performed on the z scores. First, to determine whether there is a statistically significant difference ($p<0.05$) between rats and gerbils, a three-way analysis of variance (ANOVA) was performed with species (rats, gerbils), experiment number (within species), and perturbation (within species). Afterward, to determine whether there are statistically significant differences ($p<0.05$) within animal species, between individual

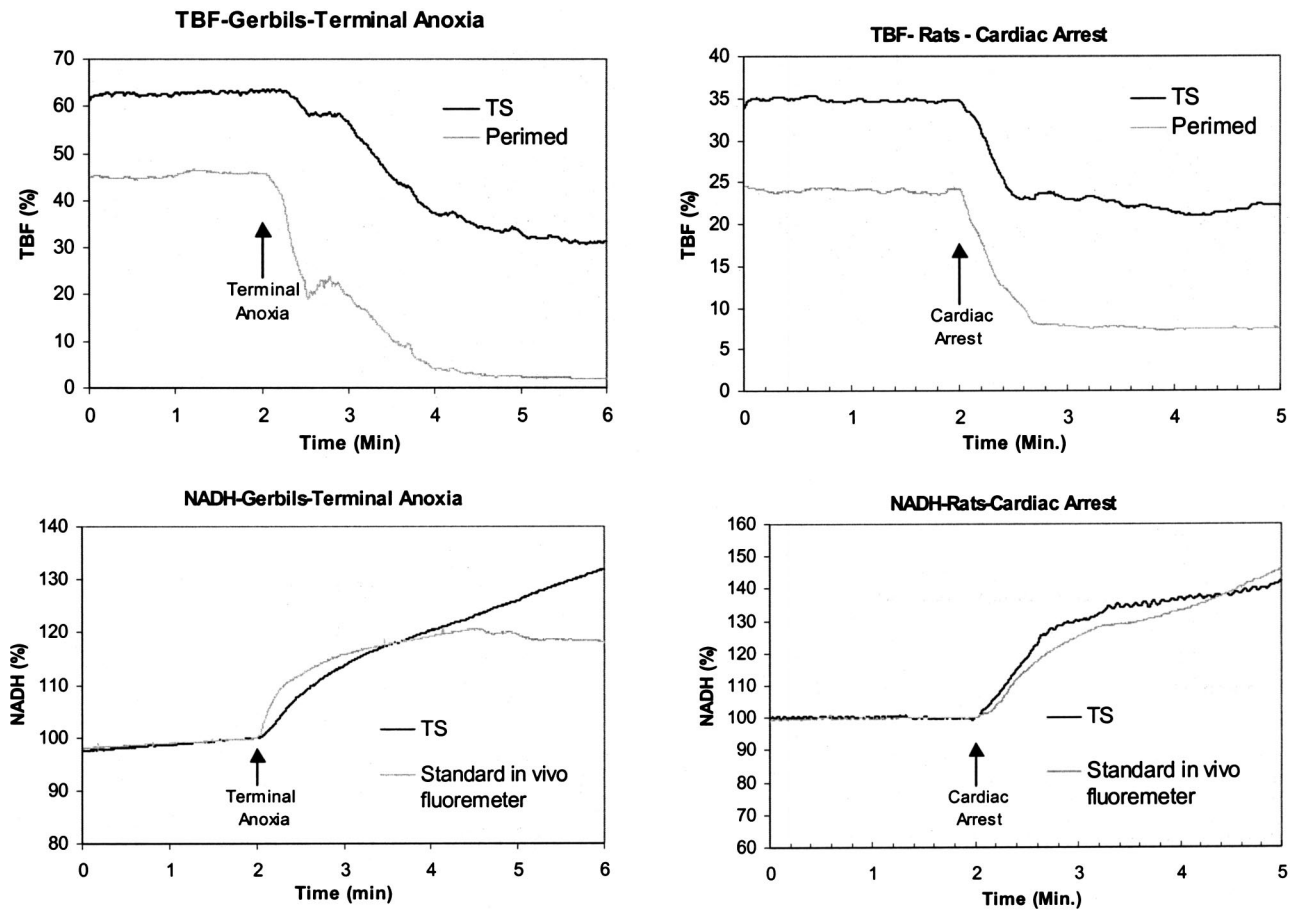


Fig. 11 Effect of terminal anoxia on the gerbil brain (on the left) and of cardiac arrest on the rat small intestine (on the right). Under both conditions, the blood flow reached its minimal level, while NADH accumulated to its maximal levels.

animals as well as between different perturbations, a two-way ANOVA was performed within each species separately, with experiment number, and perturbation. Each of these analyses was performed separately for TBF and NADH. The resulting *p* values are presented in Table 2.

Using the Bonferroni method for multiple comparisons, significant differences of the transformed correlation coefficients were found between certain perturbations but not others

(correlation coefficients are shown in Fig. 12, *p* values are not shown).

Gerbils

1. *TBF*: The correlation coefficient for ischemia (0.930) is significantly different from that of anoxia (0.750). The correlation coefficient for terminal anoxia (0.866) is in between and is not significantly different from either.
2. *NADH*: At the 5% level, there is no significant difference (*p*-value=0.07). There is no difference between

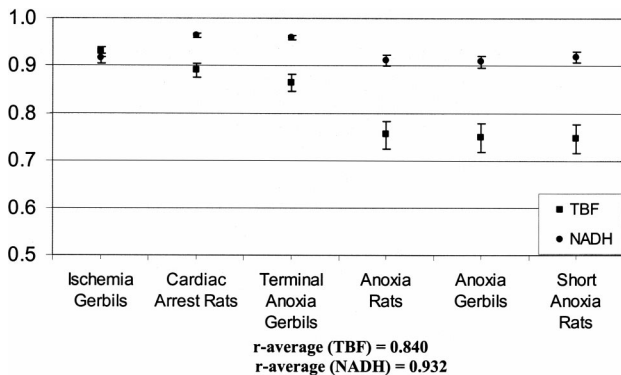


Fig. 12 Average correlation coefficients and confidence intervals of TBF and NADH for all six perturbations (rats and gerbils).

Table 2 Two/three way ANOVA and the resulting *p* values for TBF and NADH.

Source	TBF <i>p</i> value	NADH <i>p</i> value
Between species	0.11	0.63
Gerbils—between subjects	0.88	0.82
Gerbils—between perturbations	0.002	0.007
Rats—between subjects	0.37	0.20
Rats—Between perturbations	0.01	0.02

ischemia (0.916) and anoxia (0.909), but there seems to be a difference, although not statistically significant, between these and terminal anoxia (0.960).

Rats

1. *TBF*: There is no significant difference between the correlation coefficients for anoxia (0.756) and short anoxia (0.749), but there is a significant difference between these and cardiac arrest (0.892).
2. *NADH*: The correlation coefficient for cardiac arrest (0.965) is significantly different from that of anoxia (0.913). The correlation coefficient for short anoxia (0.920) is in-between and is not significantly different from either.

5 Discussion

The TS described in this paper is designed to provide the clinicians with a new device whereby tissue vitality could be assessed by real-time monitoring of three physiological parameters. To discuss the advantages of the TS, it is important to discuss other techniques available to the clinicians today. In view of the general aim to utilize the TS as a medical device, it was important to prove its performance under *in vitro* as well as *in vivo* conditions. Note that there is as yet no device for monitoring tissue vitality at the tissue level available on the clinical market.

5.1 Measurements of NADH in Solution

Several investigators have measured the fluorescence of NADH in solution. Our findings are very similar to their previous work. Very recently, Cordeiro et al.⁸¹ plotted a calibration curve for NADH fluorescence in solutions (340-nm excitation). They found a high degree of correlation ($r^2 = 0.986$). Orr and Arthurs⁸² also showed a good correlation between NADH concentration (355-nm excitation) and fluorescence intensity. White and Wittenberg⁸³ found a significant linear correlation between the percentage of NADH in a mixture with NAD and the fluorescence intensity.

In this study, both instruments, the TS and Victor², provide fluorescence outputs proportionate to NADH concentration, with correlations very close to 1.0. This shows that, in fact, the relationship to the NADH concentration is, quite expectedly, highly linear for each instrument.

The correlation between these two instruments is also close to unity, thus unequivocally establishing similarity and even equivalence between them.

5.2 In Vivo Measurements

The results shown in Figs. 10 and 11 provide a good demonstration of how the TS measurements are correlated to standard, well-characterized physiological responses. All measurements by the TS correlate well with the Periflux 2B (TBF) and the standard research fluorometer (NADH), with an average correlation coefficient of $r = 0.84$ for TBF and $r = 0.93$ for NADH. By yielding high correlation coefficients for all groups, the results unequivocally demonstrate the qualitative similarity between the TS, the Periflux and the accepted *in vivo* research fluorometer, when used in different physiological conditions as well as in different tissues and animal spe-

cies. No difference was found between the various instruments. Note that the use of either of these devices diminishes the need for absolute values in the two LDF systems. One of the main reasons for the difference in the response amplitude lies in the depth of penetration by the two wavelengths: 632 nm of the Perimed versus 325 nm of the TS. Consequently, the sampled tissue volume is not the same. Because of this, only correlation analysis can be adequate. The difference between the sensitivity of the two instruments arises for the same reason. The sampled volume is very different, as also the size of the blood vessels analyzed by the two instruments. We were able to adjust the gain of the instruments so that they would resemble each other, but since only correlation analysis was planned we left it as is.

As seen in Table 2, based on the variance analysis, there is no statistically significant difference between the correlation coefficients for animals of the same species or different species, or within a given type of perturbation. There is a statistically significant difference between the correlation coefficients for different types of perturbations, as should be expected since different metabolic perturbations induce different physiological responses.

Since all the responses to any of the perturbations are measured simultaneously by the same two devices, i.e., the TS and Periflux, or the TS and the research fluorometer, it might be expected that all the groups would have similar correlation coefficients. Nevertheless, we find differences between the correlations of different perturbations. This is understandable, however, since the physiological responses are slightly different for different perturbations. As a result of the difference in physiological responses, including autoregulatory effects on local blood flow, it can be expected that the correlation between the measured signal at two adjacent sites would be more similar for certain perturbations than for others. Similarly, when autoregulatory mechanisms are active, for example, in anoxia and short anoxia, variations in blood flow at different tissue sites can be expected.

We induced a variety of perturbations. Although all of them affect the vascular system, there are nevertheless differences between them. Some of the disturbances are systemic and affect the entire body (i.e., anoxia, when the animal breathes oxygen-deficient air, short anoxia, and terminal anoxia), while other perturbations are local (i.e., ischemia, when the arteries transporting blood to the tissue are occluded and the effect is localized to the tissue).

Additionally, the intensity of the perturbation effect depends on both its duration and nature. Duration is significant insofar as autoregulatory mechanisms are more active during a short perturbation and counteract the unwanted disturbance, whereas after a while (a few seconds) their ability to act decreases dramatically. The nature of the perturbation is significant insofar as transient or nonradical perturbations, such as anoxia or short anoxia, affect the vascular system in a lesser degree than an extreme or even terminal event, such as ischemia or terminal anoxia. The more drastic the effect on the body, the less able are the autoregulatory mechanisms to remedy the situation. For that reason, for example, the few cases of low correlation coefficients in gerbils were all seen in anoxia but not in ischemia. Anoxia is a less drastic intervention (less oxygen is supplied but continuous blood flow is main-

tained), when compared to ischemia, which is a complete arrest of cerebral blood flow.

The results show that for NADH, all correlation coefficients are above 0.9, and for TBF, they are all about 0.75 for nonradical perturbations and about 0.9 for extreme events. These results are consistent among animals of the same and different species. The very few cases where a low correlation coefficient was found are doubtlessly due to differences in the local behavior of the vascular bed, that is, if one probe is located above a tiny blood vessel and the other is not.

The results of the comparison between different sites in the same tissue, different tissues and different species emphasize the ability of the TS to measure all types of living tissue.

The effects of three types of systemic perturbations were applied on rats: "short anoxia," "anoxia," and "cardiac arrest." "Anoxia" is defined as "absence or almost complete absence of oxygen from inspired gases, arterial blood, or tissues."⁸⁴ Introduction of changes in the oxygen content of the inhaled air is an effective, easy and reliable way to affect the blood flow of various organs, without further interference with the normal function of the organism, such as intravenous catheterization or introduction of chemicals to the body.

The perturbations applied on gerbils were "anoxia," "ischemia," and "terminal anoxia." "Ischemia" is defined as "local anemia due to mechanical obstruction (mainly arterial narrowing) of the blood supply"⁸⁵ and was achieved by occlusion of the arteries transporting blood to the brain. The unique anatomy of the incomplete Willis circle, peculiar only to gerbils, permits a total cerebral blockade of the blood supply.³⁶

The effects of the above mentioned perturbations on the TBF and NADH in the brain and intestine are well documented.^{84,86-88} Briefly, short anoxia, anoxia, and terminal anoxia, all cause a decrease in the blood flow, transient or terminal, in both the TBF of the brain and intestine. Ischemia causes the same TBF effect in the brain, and an increase in NADH level. The NADH signal increases in a mono- or bi-phasic manner when the brain or intestine is exposed to anoxia.

5.2.1 Variations in blood flow in different sites of the same tissue

Variations in the blood flow in different sites of the same tissue are very low, and are characterized by the coefficient of variation.^{89,90} The coefficient of variation relates to the extent of the homogeneity of the vascular bed anatomy and the capillary density of a certain tissue, that is to say how similar the blood flow is when measured at different sites of the same tissue. For example, the coefficients of variation are 25% for the skin, 15% for the small intestine, 33% for the stomach, and 34% for the gracilis muscle. In an earlier study, simultaneous measurements of TBF (by the Perimed) and NADH (by the standard *in vivo* research fluorometer) from 4 sites of the rat brain cortex were performed.⁹¹ The tendencies in the different sites are considerably similar with regard to the kinetics and amplitude when visually assessed (no statistical data available).

The magnitude of the TBF signal depends on a number of factors that probably differ between tissues, e.g., hematocrit,

RBC (red blood cells) velocity, vascular geometry, tissue optical properties, and point-to-point variations of the blood flow within the tissue. These differences might prevent the calibration factors obtained in one vascular bed from being applied to another, meaning that the baseline levels of the blood flow in different tissues cannot be compared due to those factors. However, the methodology of inducing a change and measuring the net response, minimizes the influence of those factors. For this reason, to compare the devices despite those variations, we applied perturbations and measured the changes simultaneously by both devices, rather than the baseline TBF values.

5.2.2 Different tissues

Two types of organs were used to broaden the range of tissues measured. The brain is one of the primary organs whose blood flow and activity are of the highest importance for the survival of the organism. The intestine represents an internal organ, which belongs to the supporting systems. Its blood flow and function are necessary but not crucial for the immediate survival of the organism.²⁰

5.2.3 Different animals

Two kinds of animals were used (gerbils and rats). The measurements performed by the TS, such as LDF, tissue reflectance and NADH fluorescence, are based on the physical and physiological properties, common to most mammalian species and almost all types of tissue, such as autoregulated blood flow and oxygen dependency, the tissue composition of cells and blood capillaries, etc. The conception of the "identical principles of physiological function between different organisms" is the rationale behind the claim of the TS efficiency in any living tissue.⁹²

Since both instruments conduct the measurements simultaneously, the variations resulting from different types of tissue, or different animal species, are detected by both instruments in a similar manner. Therefore, the comparison is indeed valid. Furthermore, the variations are minimized by the large sample size (15 repetitions in the average for each perturbation).

5.3 Conclusions

In the initial pilot study, the TS, when compared to the Periflux and the accredited *in vivo* research fluorometer, was found to be essentially equivalent. Further studies are required to prove its general clinical applicability. The results of comparison, obtained in the pilot study, between different sites in the same tissue, different tissues, and different species, confirm the ability of the TS to be broadly applied in the future. The TS performance is consistent in different species and different tissues, thus attesting that the experimental model constitutes a valid representation of all mammalian tissue.

Acknowledgments

We thank and acknowledge Dr. Y. Kamenir of Bar-Ilan University for help with the statistical analysis, and I. Stembler of Bar-Ilan University for editorial assistance.

References

- J. Boldt, "Clinical review: hemodynamic monitoring in the intensive care unit," *Clin. Crit. Care Med.* **6**, 52–59 (2002).
- M. P. Fink, "Cytopathic hypoxia. Is oxygen use impaired in sepsis as a result of an acquired intrinsic derangement in cellular respiration?" *Crit. Care Clin.* **18**, 165–175 (2002).
- B. Chance, N. Oshino, T. Sugano, and A. Mayevsky, "Basic principles of tissue oxygen determination from mitochondrial signals," in *Oxygen Transport to Tissue. Instrumentation, Methods, and Physiology*, H. I. Bicher and D. F. Bruley, Eds., pp. 277–292, Plenum, New York (1973).
- K. Wardell, I. M. Braverman, D. G. Silverman, and G. E. Nilsson, "Spatial heterogeneity in normal skin perfusion recorded with laser Doppler imaging and flowmetry," *Microvasc. Res.* **48**, 26–38 (1994).
- G. F. Clough, A. R. Bennett, and M. K. Church, "Effects of H1 antagonists on the cutaneous vascular response to histamine and bradykinin: a study using scanning laser Doppler imaging," *Br. J. Dermatol.* **138**, 806–814 (1998).
- F. F. Jobsis, "Noninvasive, infrared monitoring of cerebral and myocardial oxygen sufficiency and circulatory parameters," *Science* **198**, 1264–1267 (1977).
- A. Villringer and B. Chance, "Non-invasive optical spectroscopy and imaging of human brain function," *Trends Neurosci.* **20**, 435–442 (1997).
- A. Villringer, J. Planck, C. Hock, L. Schleinkofer, and U. Dirnagl, "Near infrared spectroscopy (NIRS): a new tool to study hemodynamic changes during activation of brain function in human adults," *Neurosci. Lett.* **154**, 101–104 (1993).
- U. Dirnagl, B. Kaplan, M. Jacewicz, and W. Pulsinelli, "Continuous measurement of cerebral cortical blood flow by Laser Doppler Flowmetry with a rat stroke model," *J. CBF Metab.* **9**, 589–596 (1989).
- R. L. Haberl, M. L. Heizer, A. Marmarou, and E. F. Ellis, "Laser Doppler assessment of brain microcirculation: effect of systemic alterations," *Am. J. Physiol.* **256**, H1247–H1254 (1989).
- J. Dings, A. Jager, J. Meixensberger, and K. Roosen, "Brain tissue pO₂ and outcome after severe head injury," *Neurol. Res.* **20**(Suppl 1:S71-5), S71–S75 (1998).
- K. H. Frank, M. Kessler, K. Appelbaum, and W. Dumlner, "The Erlangen micro-lightguide spectrophotometer EMPHO I," *Phys. Med. Biol.* **34**, 1883–1900 (1989).
- I. J. Rampil, L. Litt, and A. Mayevsky, "Correlated, simultaneous, multiple-wavelength optical monitoring *in vivo* of localized cerebrocortical NADH and brain microvessel hemoglobin oxygen saturation," *J. Clin. Monit.* **8**, 216–225 (1992).
- B. Chance and G. R. Williams, "Respiratory enzymes in oxidative phosphorylation. I. Kinetics of oxygen utilization," *J. Biol. Chem.* **217**, 383–393 (1955).
- A. Mayevsky and B. Chance, "A new long-term method for the measurement of NADH fluorescence in intact rat brain with implanted cannula," in *Proc. Int. Symp. on Oxygen Transport to Tissue. Adv. Exp. Med. Biol.*, pp. 239–244, Plenum Press, New York (1973).
- M. Rosenthal and F. F. Jobsis, "Intracellular redox changes in functioning cerebral cortex. II. Effects of direct cortical stimulation," *J. Neurophysiol.* **34**, 750–762 (1971).
- E. Dora, "A simple cranial window technique for optical monitoring of cerebrocortical microcirculation and NAD/NADH redox state. Effect of mitochondrial electron transport inhibitors and anoxic anoxia," *J. Neurochem.* **42**, 101–108 (1984).
- E. Dora, L. Gyulai, and A. G. B. Kovach, "Determinants of brain activation-induced cortical NAD/NADH responses *in vivo*," *Brain Res.* **299**, 61–72 (1984).
- F. F. Jobsis, M. O'Connor, A. Vitale, and H. Vreman, "Intracellular redox changes in functioning cerebral cortex. I. Metabolic effects of epileptiform activity," *Neurophysiology* **34**, 735–749 (1971).
- A. Mayevsky and B. Chance, "Intracellular oxidation reduction state measured *in situ* by a multichannel fiber-optic-surface fluorometer," *Science* **217**, 537–540 (1982).
- A. Mayevsky, "Brain NADH redox state monitored *in vivo* by fiber optic surface fluorometry," *Brain Res. Rev.* **7**, 49–68 (1984).
- P. Shepherd and P. A. Oberg, *Laser Doppler Blood Flowmetry*, Kluwer Academic, Naswell USA, (1990).
- R. Bonner and R. Nossal, "Model for laser Doppler measurements of blood flow in tissue," *Appl. Opt.* **20**, 2097–2107 (1981).
- A. Javan, W. R. Bennett, and D. R. Herriott, "Population inversion and continuous optical laser oscillation in a gas discharge containing a He-Ne mixture," *Phys. Rev. Lett.* **6**, 106–110 (1961).
- Y. Yeh and H. Cummins, "Localized fluid flow measurements with an He-Ne laser spectrometer," *Appl. Phys. Lett.* **4**, 176–178 (1964).
- C. Riva, B. Ross, and G. B. Benedek, "Laser Doppler measurements of blood flow in capillary tubes and retinal arteries," *Invest. Ophthalmol.* **11**, 936–944 (1972).
- M. D. Stern, "In vivo evaluation of microcirculation by coherent light scattering," *Nature (London)* **254**, 56–58 (1975).
- M. D. Stern, D. L. Lappe, P. D. Bowen, J. E. Chimosky, G. A. Holloway, and H. R. Keiser, "Continuous measurement of tissue blood flow by Laser Doppler spectroscopy," *Am. J. Physiol.* **232**, H441–H448 (1977).
- P. A. Oberg, "Laser-Doppler flowmetry," *Crit. Rev. Biomed. Eng.* **18**, 125–163 (1990).
- A. N. Obeid, G. Dougherty, and S. Pettinger, "In vivo comparison of a twin wavelength laser Doppler flowmeter using He-Ne and laser diode sources," *J. Med. Eng. Technol.* **14**, 102–110 (1990).
- M. D. Stern, P. D. Bowen, R. Parma, R. W. Osgood, R. L. Bowman, and J. H. Stein, "Measurement of renal cortical and medullary blood flow by laser-Doppler spectroscopy in the rat," *Hokkaido Math. J.* **236**, F80–F87 (1979).
- G. Belcaro, U. Hoffmann, A. Bollinger, and A. Nicolaidis, *Laser Doppler*, Med-Orion Publishing, London, Los-Angeles, Nicosia (1994).
- N. Vongsavan and B. Matthews, "Some aspects of the use of laser Doppler flow meters for recording tissue blood flow," *Exp. Physiol.* **78**, 1–14 (1993).
- A. Mayevsky, K. Frank, M. Muck, S. Nioka, M. Kessler, and B. Chance, "Multiparametric evaluation of brain functions in the Mongolian gerbil *in vivo*," *J. Basic Clin. Physiol. Pharmacol.* **3**, 323–342 (1992).
- A. Mayevsky, "Cerebral blood flow and brain mitochondrial redox state responses to various perturbations in gerbils," in *Oxygen Transport to Tissue XIV*, W. Erdmann, Ed., pp. 707–716, Plenum Press, New York, London (1992).
- A. Mayevsky, E. Yoles, N. Zarchin, and D. Kaushansky, "Brain vascular ionic and metabolic responses to ischemia in the Mongolian gerbil," *J. Basic Clin. Physiol. Pharmacol.* **1**, 207–220 (1990).
- A. Mayevsky, E. S. Flamm, W. Pennie, and B. Chance, "A fiber optic based multiprobe system for intraoperative monitoring of brain functions," *Proc. SPIE* **1431**, 303–313 (1991).
- A. Mayevsky, A. Doron, T. Manor, S. Meilin, N. Zarchin, and G. E. Ouaknine, "Cortical spreading depression recorded from the human brain using a multiparametric monitoring system," *Brain Res.* **740**, 268–274 (1996).
- D. W. Lubbers, "Optical sensors for clinical monitoring," *Acta Anaesthesiol. Scand., Suppl.* **39**, 37–54 (1995).
- B. Chance and H. Baltscheffsky, "Respiratory enzymes in oxidative phosphorylation," *J. Biol. Chem.* **233**, 736–739 (1958).
- B. Chance, B. Schoener, R. Oshino, F. Itshak, and Y. Nakase, "Oxidation-reduction ratio studies of mitochondria in freeze-trapped samples. NADH and flavoprotein fluorescence signals," *J. Biol. Chem.* **254**, 4764–4771 (1979).
- A. P. Koretsky and R. S. Balaban, "Changes in pyridine nucleotide levels alter oxygen consumption and extra-mitochondrial phosphates in isolated mitochondria: a ³¹P-NMR and NAD(P)H fluorescence study," *Biochim. Biophys. Acta* **893**, 398–408 (1987).
- T. Galeotti, G. D. V. van Rossum, D. Mayer, and B. Chance, "Spectrofluorimetric detection of 'free' and 'bound' forms of NAD(P)H in normal and tumoral cells," in *Atti del Seminario di Studi Biologici*, E. Quagliariello, Ed., pp. 249–270, Adriatica Editrice, Bari (1969).
- E. Kohen, C. Kohen, and B. Thorell, "Use of microfluorimetry to study the metabolism of intact cells," *Biomed. Eng.* **4**, 554–565 (1969).
- J. Eng, R. M. Lynch, and R. S. Balaban, "Nicotinamide adenine dinucleotide fluorescence spectroscopy and imaging of isolated cardiac myocytes," *Biophys. J.* **55**, 621–630 (1989).
- B. Chance, P. Cohen, F. Jobsis, and B. Schoener, "Intracellular oxidation-reduction states *in vivo*," *Science* **137**, 499–508 (1962).
- D. J. Pappajohn, R. Penneys, and B. Chance, "NADH spectrofluorimetry of rat skin," *J. Appl. Physiol.* **33**, 684–687 (1972).
- A. P. Koretsky, L. A. Katz, and R. S. Balaban, "Determination of pyridine nucleotide fluorescence from the perfused heart using an internal standard," *Am. J. Physiol.* **253**, H856–H862 (1987).
- B. Chance, "Biochemical studies of transitions from rest to activity,"

- V in Sleep and Altered States of Consciousness*, pp. 48–63, The Williams & Wilkins Company, Baltimore, (1967).
50. T. M. Sundy and R. E. Anderson, "Reduced nicotinamide adenine dinucleotide fluorescence and cortical blood flow in ischemic and nonischemic squirrel monkey cortex. I. Animal preparation, instrumentation, and validity of model," *Stroke* **6**, 270–278 (1975).
 51. K. Harbig, B. Chance, A. G. B. Kovach, and M. Reivich, "In vivo measurement of pyridine nucleotide fluorescence from cat brain cortex," *J. Appl. Physiol.* **41**, 480–488 (1976).
 52. B. Chance, "Pyridine nucleotide as an indicator of the oxygen requirements for energy-linked functions of mitochondria," *Circ. Res.* **38**, 1-31–1-37 (1976).
 53. M. J. O'Connor, D. V. Lewis, and C. J. Herman, "Effects of potassium on oxidative metabolism and seizures," *Electroencephalogr. Clin. Neurophysiol.* **35**, 205–208 (1973).
 54. M. Rosenthal and G. Somjen, "Spreading depression of cerebral cortex of cats," *J. Neurophysiol.* **36**, 739–749 (1973).
 55. F. F. Jobsis, J. H. Keizer, J. C. LaManna, and M. Rosenthal, "Reflectance spectrophotometry of cytochrome aa3 in vivo," *J. Appl. Physiol.* **43**, 858–872 (1977).
 56. J. C. LaManna, G. Watkins, and M. Rosenthal, "Relationship of inspired oxygen level of cytochrome a and ECoG in cats," *Physiologist* **18**, 284 (1975).
 57. M. Rosenthal, J. C. LaManna, F. F. Jobsis, J. E. Levasseur, H. A. Kontos, and J. L. Patterson, "Effects of respiratory gases on cytochrome A in intact cerebral cortex: is there a critical Po₂?" *Brain Res.* **108**, 143–154 (1976).
 58. B. Chance, A. Mayevsky, C. Goodwin, and L. Mela, "Factors in oxygen delivery to tissue," *Microvasc. Res.* **8**, 276–282 (1974).
 59. J. T. Cummins and H. W. Elliott, "Effect of morphine on the potassium-induced change in the level of reduced pyridine nucleotides and cytochromes in brain slices," *Biochem. Pharmacol.* **25**, 893–896 (1976).
 60. R. S. Balaban and L. J. Mandel, "Coupling of aerobic metabolism to active ion transport in the kidney," *J. Physiol. (London)* **304**, 331–348 (1980).
 61. R. S. Balaban, L. J. Mandel, S. P. Soltoff, and J. M. Storey, "Coupling of active ion transport and aerobic respiratory rate in isolated renal tubules," *Proc. Natl. Acad. Sci. U.S.A.* **77**, 447–451 (1980).
 62. H. Franke, C. H. Barlow, and B. Chance, "Surface fluorescence of reduced pyridine nucleotide of the perfused rat kidney: interrelation between metabolic and functional states," *Contrib Nephrol.* **19**, 240–247 (1980).
 63. R. S. Balaban and J. J. Blum, "Hormone-induced changes in NADH fluorescence and O₂ consumption of rat hepatocytes," *Am. J. Physiol.* **242**, C172–C177 (1982).
 64. S. Ji, J. J. Lemasters, and R. G. Thurman, "A non-invasive method to study metabolic events within sublobular regions of hemoglobin-free perfused liver," *FEBS Lett.* **113**, 37–41 (1980).
 65. T. Kitai, A. Tanaka, A. Tokuka, K. Ozawa, S. Iwata, and B. Chance, "Changes in the redox distribution of rat liver by ischemia," *Anal. Biochem.* **206**, 131–136 (1992).
 66. J. Kedem, A. Mayevsky, J. Sonn, and B. A. Acad, "An experimental approach for evaluation of the O₂ balance in local myocardial regions in vivo," *Q. J. Exp. Physiol.* **66**, 501–514 (1981).
 67. C. Ince, J. F. Ashruf, J. A. M. Avontuur, P. A. Wieringa, J. A. E. Spaan, and H. A. Bruining, "Heterogeneity of the hypoxic state in rat heart is determined at capillary level," *Am. J. Physiol.* **264**, H294–H301 (1993).
 68. G. Renault, E. Raynal, M. Sinet, M. Muffat-Joly, J.-P. Berthier, J. Cornillault, B. Godard, and J.-J. Pocardalo, "In situ double-beam NADH laser fluorimetry: choice of a reference wavelength," *Am. J. Physiol.* **246**, H491–H499 (1984).
 69. F. F. Jobsis, M. J. O'Connor, M. Rosenthal, and J. M. VanBuren, "Fluorometric monitoring of metabolic activity in the intact cerebral cortex," 253 in *Neurophysiology Studied in Man*, pp. 18–26, Excerpta Medica, Amsterdam (1971).
 70. A. Mayevsky and B. Chance, "Repetitive patterns of metabolic changes during cortical spreading depression of the awake rat," *Brain Res.* **65**, 529–533 (1974).
 71. S. Ji, B. Chance, B. H. Stuart, and R. Nathan, "Two-dimensional analysis of the redox state of the rat cerebral cortex in vivo by NADH fluorescence photography," *Brain Res.* **119**, 357–373 (1977).
 72. A. Mayevsky and B. Chance, "The effect of decapitation on the oxidation-reduction state of NADH and ECoG in the brain of the awake rat," in *Oxygen Transport to Tissue II, Adv. Exp. Med. Biol.*, pp. 307–312 (1976).
 73. A. Mayevsky, "Ischemia in the brain: The effects of carotid artery ligation and decapitation on the energy state of the awake and anesthetized rat," *Brain Res.* **140**, 217–230 (1978).
 74. A. Mayevsky and N. Zarchin, "The effects of unilateral carotid occlusion on the responses to decapitation in the gerbil brain," *Brain Res.* **206**, 155–160 (1981).
 75. N. Zarchin and A. Mayevsky, "The effects of age on the metabolic and electrical responses to decapitation in the awake and anesthetized rat brain," *Mech. Ageing Dev.* **16**, 285–294 (1981).
 76. A. Mayevsky, "Level of ischemia and brain functions in the Mongolian gerbil in vivo," *Brain Res.* **524**, 1–9 (1990).
 77. G. E. Nilsson, T. Tenland, and P. A. Obert, "A new instrument for continuous measurement of tissue blood flow by light beating spectroscopy," *IEEE Trans. Biomed. Eng.* **27**, 12–19 (1980).
 78. J. M. Bland and D. G. Altman, "Statistical methods for assessing agreement between two methods of clinical measurement," *Lancet* **1**, 307–310 (1986).
 79. J. M. Bland and D. G. Altman, "Comparing methods of measurement: why plotting difference against standard method is misleading," *Lancet* **346**, 1085–1087 (1995).
 80. A. Mayevsky, N. Zarchin, and C. M. Friedli, "Factors affecting the oxygen balance in the awake cerebral cortex exposed to spreading depression," *Brain Res.* **236**, 93–105 (1982).
 81. P. G. Cordeiro, R. E. Kirschner, Q.-Y. Hu, J. J. C. Chiao, H. Savage, R. R. Alfano, L. A. Hoffman, and D. A. Hidalgo, "Ultraviolet excitation fluorescence spectroscopy: A noninvasive method for the measurement of redox changes in ischemic myocutaneous flaps," *Plast. Reconstr. Surg.* **96**, 673–680 (1995).
 82. C.-S. Orr and S. C. Arthurs, "Tissue viability measurement by *in situ* fluorometry," *ASAIO Trans.* **38**, M412–M415 (1992).
 83. R. L. White and B. A. Wittenberg, "NADH fluorescence of isolated ventricular myocytes: effects of pacing, myoglobin, and oxygen supply," *Biophys. J.* **65**, 196–204 (1993).
 84. D. K. Von Lubitz, R. C. Lin, and K. A. Jacobson, "Cerebral ischemia in gerbils: effects of acute and chronic treatment with adenosine A_{2A} receptor agonist and antagonist," *Eur. J. Pharmacol.* **287**, 295–302 (1995).
 85. M. Spraycar, *Stedman's Medical Dictionary*, Williams & Wilkins, Baltimore (1995).
 86. E. Dora, "Effect of 'flow anoxia' and 'non flow anoxia' on the NAD/NADH redox state of the intact brain cortex of the cat," *Pflugers Arch. Eur. J. Physiol.* **405**, 148–154 (1985).
 87. M. Kaminogo, "Changes of cortical oxidative metabolism and cortical oxygen tension in hypoxia, anoxia and ischaemia," *Neurol. Res.* **11**, 139–144 (1989).
 88. R. E. Anderson and T. M. Sundt, Jr., "Instrumentation for *in vivo* cerebral NADH studies in squirrel monkey," *IEEE Trans. Biomed. Eng.* **BME-22**, 220–224 (1975).
 89. D. J. Godden, E. M. Baile, and P. D. Pare, "A comparison of laser Doppler flowmetry with the radiolabelled microsphere reference flow technique to measure tracheal blood flow in dogs," *Acta Physiol. Scand.* **142**, 49–57 (1991).
 90. G. J. Smits, R. J. Roman, and J. H. Lombard, "Evaluation of laser-Doppler flowmetry as a measure of tissue blood flow," *J. Appl. Physiol.* **61**, 666–672 (1986).
 91. T. Manor, A. Meilin, and A. Mayevsky, "Monitoring different areas of the rat cortex in response to fluid percussion trauma," *Isr J. Med. Sci.* **32(Suppl.)**, S39 (1996).
 92. A. Kraut, Y. Zurovsky, and A. Mayevsky, "Simultaneous hemodynamic and metabolic responses to oxygen deficiency in the brain and other organs of the rat," *Neurosci. Lett. Suppl.* **51**, S24 (1998) (Abstract).